# Structural Analysis of Phospholipase $A_2$ from Functional Perspective. 2. Characterization of a Molten Globule-Like State Induced by Site-Specific Mutagenesis†

Chunhua Yuan,‡ In-Ja L. Byeon,§ Ming-Jye Poi,|| and Ming-Daw Tsai*,‡,§,||,⊥

*Departments of Chemistry and Biochemistry, Campus Chemical Instrument Center, and Ohio State Biochemistry Program, The Ohio State University, Columbus, Ohio 43210*

*Received September 14, 1998; Revised Manuscript Received December 17, 1998*

ABSTRACT: Previous NMR studies have shown that many phospholipase $A_2$ (PLA2, from bovine pancreas, overexpressed in *Escherichia coli*) mutants display some properties reminiscent of a molten globule state. Further NMR analyses for some of the mutants indicated that formation of the "molten globule-like state" is a pH-dependent phenomenon. The mutants I9Y and I9F showed perturbed NMR properties throughout the pH range studied, while the mutants H48A and C44A/C105A displayed native-like spectra at neutral pH but molten globule-like ones under acidic conditions, with a "transition pH" around 4. On the other hand, wild-type PLA2 exhibits exceptional pH stability and turns into a similar molten globule-like state only under highly acidic conditions such as 1 M HCl. The H48A mutant was used to rigorously establish the property of the molten globule-like state of PLA2 mutants. The results of far-UV CD, near-UV CD, and ANS-binding fluorescence suggest that H48A retains native-like secondary structures but loses tertiary structure during the conformational transition. However, the tertiary structure is not completely lost, as evidenced by the retention of some long-range NOEs in two-dimensional NOESY spectra. The conclusion was further substantiated by three-dimensional NOESY−HSQC experiments on a $^{15}N$-labeled H48A sample. It was revealed that the molten globule-like state at mildly acidic pH retained some rigid tertiary structure, which consisted of partial α-helix II (Y52−L58), α-helix III (D59−V63), *β*-wing (S74−S85) and partial α-helix IV (A90−N97). These residual tertiary structures grouped in half of the protein could be attributed to stabilization by some of the disulfide bonds. The extreme sensitivity of the PLA2 structure to site-directed mutagenesis is unprecedented. It is interesting to note that most of the functional residues (the active site, the hydrophobic channel, the interfacial binding site, and the calcium-binding loop) are located in the remainder of the protein, which is well disrupted in tertiary interactions.

Bovine pancreatic phospholipase $A_2$ (PLA2[1]) is a small globular protein consisting of only 123 amino acids ($M_r$ = 13.8 kDa). We have recently determined the high-resolution solution structure of wild-type (WT) PLA2 at a neutral pH (*1*), and analyzed it in comparison with the X-ray crystal structure (*2*, *3*). As shown in Figure 1, this protein has seven disulfide bridges as well as rich secondary elements: α-helices I (W3−I13), II (D40−L58), III (D59−V63), IV (A90−K108), and antiparallel *β*-wings (S74−S78 and E81−S85). It is thermally and chemically stable. For example, it can sustain heating at 70 °C for about 30 min during the preparation of deuterium-exchanged NMR samples (*4*), and it is not denatured by guanidinium chloride at the saturated concentration of 8 M in the presence of $Ca^{2+}$ (*5*).

Considering all of the features of stability, one would expect PLA2 to be resistant to structural perturbations caused by point mutations. However, we have reported that it was unusually easy to convert this protein into a molten globule-like state by mutagenesis, which dates back to a preliminary communication in 1992 (*6*). Since then, mutants found having this behavior include L2R, L2W, Q4K, F5A, F5V, N6A, I9Y and I9F (*7*, *8*), H48A and H48N (*9*), Y73S, Y73A, Y73K, Y73F and Y52F/Y73F (*10*, *11*), D99N, D99A (*6*, *11*), C44A/C105A and C11A/C77A (*12*), and D99N/Y52F/Y73F (*13*). Most of these mutants were designed to test the functional roles of the mutated residues, which are part of the active site, the interfacial binding site, the hydrophobic channel, or the hydrogen-bonding network. The finding of the structural roles of these residues was serendipitous.

† This work was supported by NIH Grant GM 41788 to M.-D.T. The study made use of a Bruker DMX-600 NMR spectrometer at The Ohio State University funded by NIH Grant RR 08299 and NSF Grant BIR-9221639.

* To whom correspondence should be addressed at the Department of Chemistry, The Ohio State University, 100 West 18th Avenue, Columbus, OH 43210-1173. Telephone: (614) 292-3080. FAX: (614) 292-1532. E-mail: Tsai.7@osu.edu.

‡ Department of Chemistry.

§ Campus Chemical Instrument Center.

|| Ohio State Biochemistry Program.

⊥ Department of Biochemistry.

[1] Abbreviations: 1D, one-dimensional; 2D, two-dimensional; 3D, three-dimensional; AK, adenylate kinase; ANS, 1-anilinonaphalene-8-sulfonate; CD, circular dichroism; COSY, correlated spectroscopy; HSQC, heteronuclear single-quantum coherence; NMR, nuclear magnetic resonance; NOE, nuclear Overhauser effect; NOESY, nuclear Overhauser enhancement spectroscopy; PLA2, phospholipase $A_2$; TMSP, sodium 3-trimethyl-silylpropionate-2,2,3,3-$d_4$; UV, ultraviolet; WT, wild-type.

10.1021/bi9822123 CCC: $18.00 
Published on Web 02/17/1999

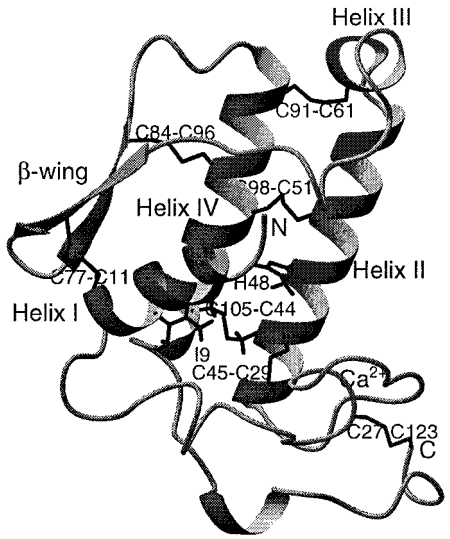


FIGURE 1: Ribbon diagram of bovine pancreatic PLA2 solution structure showing the secondary elements, seven disulfide bonds, and the mutated residues (C44, C105, I9, and H48) (*1*). The four helices are labeled as helix I, II, III, and IV. The figure was prepared using the program MOLMOL (*53*).

Typically, these mutants are characterized by broad NMR resonances, narrow chemical shift dispersion, loss of slowly exchanging NH protons, and a significant loss of NOE cross-peaks. These features from NMR experiments, along with the retention of secondary structures as indicated by far-UV CD spectra, are apparently characteristic of a molten globule state (reviewed in *14*, *15*). However, unlike classical molten globules, these PLA2 mutants still retain some fixed side chain−side chain interactions, and they still undergo cooperative denaturation induced by guanidinium chloride.

The occurrence of this conformational flexibility in PLA2 mutants is highly unusual. This phenomenon presents three challenging problems: to further characterize and define these molten globule-like states, to understand the factors stabilizing the residual structure, and to explore the structural features responsible for the high tendency toward formation of molten globule-like states upon mutation. Understanding of these problems will likely enhance the understanding of the structure−function relationship in PLA2 and provide valuable insights into the principles of structural stabilization and even the mechanism of protein folding.

This paper focuses mainly on the first problem: further characterization and definition of the molten globule-like state(s) of PLA2 mutants. This is an important step for the following reasons: (i) In all of the previous reports, the NMR analyses were performed around pH* 4.0, at which the possible microaggregation could be avoided (*8*) and the best overall resolution was achieved (*4*). It is very common to perform detailed NMR analysis of proteins at this slightly acidic condition. However, the pH effect has to be examined because it is well established that acid plays a role in the formation of molten globule states (*14*, *16*). (ii) Although the mutants mentioned above were reported to exist in a state similar to the molten globule state mainly on the basis of NMR properties, the nature of these states has not been further probed by other spectroscopic methods such as near-UV CD and fluorescence (*17*). (iii) Most importantly, the structural description of the molten globule-like state is essential for understanding the other two problems. Our recent NMR structural analysis of WT PLA2 (*1*) opens up the possibility for more detailed characterization via solution NMR (*18*).

In this paper, we first report that the formation of the molten globule-like state is a pH-dependent phenomenon and then present further characterization on its nature by far-UV CD, near-UV CD, ANS-binding fluorescence, and NMR experiments on selected mutants. We demonstrate that this conformational state induced by site-specific mutagenesis under mildly acidic conditions possesses several distinct features that characterize a molten globule, but it also retains a somewhat structured upper half. The lower half, which loses significantly the tertiary interactions, consists of most of the functional residues in PLA2 (the active site, the hydrophobic channel, the calcium-binding loop, etc).

## MATERIALS AND METHODS

*Materials.* Samples of WT, I9Y, I9F, H48A, and C44A/C105A were bovine pancreatic PLA2 mutants overexpressed in *Escherichia coli* (*19*). The mutated sites are highlighted in Figure 1. The construction of these mutants and the procedures of protein purification have been described in the Phospholipase $A_2$ Engineering series (*7*, *9*, *12*). A uniformly $^{15}N$-labeled H48A mutant was purified by growing host cells BL21(DE3)[plysS] in M9 medium with $(^{15}NH_4)_2SO_4$ as the only nitrogen source (*20*).

*NMR Spectroscopy.* All NMR experiments were carried out on a Bruker DMX-600 spectrometer equipped with a 5 mm triple-resonance probe with three-axis gradients. The experiment temperature was always set to 37 °C.

To investigate pH effect and to assign aromatic−aliphatic NOEs, the one-dimensional (1D) and two-dimensional (2D) $^1H$ NMR experiments were conducted in $D_2O$. The deuterium-exchanged samples were prepared as described previously (*9*), which typically contained about 0.7 mM enzyme, 50 mM $CaCl_2$, and 300 mM NaCl. TMSP was used as an internal chemical shift reference. The pH* was adjusted with NaOD and DCl stock solutions and measured with a micro combination glass electrode in sample preparation and during the pH titration experiment.[2] The solvent suppression was achieved by presaturation in all NMR experiments. In 2D NOESY experiments, 200-ms mixing time was used and the total acquisition time was about 15 h. A COSY experiment was performed for each sample at neutral pH* to assist assignments of aromatic spins.

$^{15}N$-Labeled and nonlabeled H48A samples were used to investigate the conformational changes associated with backbone amides. Samples containing same salts were dissolved in a 95% $H_2O$/5% $D_2O$ mixture (referred to as "$H_2O$" hereafter). For all spectra, a 3-9-19 pulse sequence (*21*) was used to suppress the water signal. 2D NOESY spectra were recorded at pH 6.0 and pH 4.0 on nonlabeled H48A with a mixing time of 200 ms. Parallel experiments were conducted on WT for the purpose of comparison. To get detailed analysis, 2D HSQC (*22*, *23*) and three-dimensional (3D) $^{15}N$-edited NOESY-HSQC (*24*) experiments were conducted at pH 6.0 and pH 4.0 on the uniformly $^{15}N$-labeled H48A mutant. Quadrature detection in the

[2] All pH values are direct measurements at 25 °C without any correction. pH* indicates the measurement in $D_2O$.

indirect dimensions was via States-time proportional phase incrementation (States-TPPI) (*25*). The 3D experiments utilized 120 ms mixing time. The sweep widths were set to 9615, 2127, and 9165 Hz for F3 ($^1$H), F2 ($^{15}$N), and F1 ($^1$H), respectively. The data matrices were 2048 (F3, $^1$H) × 64 (F2, $^{15}$N) × 256 (F1, $^1$H), with total acquisition time about 90 h. Both F1 and F2 indirect dimensions were weighted by a 90° shifted squared sinebell window function, and the acquisition dimension (F3) was zero-filled to 4096 complex points followed by application of the Gaussian window function.

Data were processed with XWINNMR software (ver. 2.0, Bruker) installed on Silicon Graphics workstations. The assignments were made on the basis of total chemical shift assignment on WT PLA2 at pH 6.0 (*1*).

*CD Spectroscopy.* CD spectra were collected on a JASCO J-500C spectropolarimeter using a quartz microcell of 1-cm length. The measurements were carried out at 37 °C in a thermostatically controlled cell holder. The samples for the far-UV CD experiment contained 5.3 $\mu$M enzyme, 30 mM NaCl, and 10 mM $CaCl_2$ in double distilled water, and the samples for the near-UV CD experiment contained 0.13 mM protein, 300 mM NaCl, and 50 mM $CaCl_2$. The pH was adjusted with NaOH and HCl stock solutions. The CD experimental conditions were 20 nm/min, step resolution 0.2 nm, bandwidth 2.0 nm, 2−4 scans for each run. The data were saved and then processed in commercial graphics software with curve smoothing. Mean residue ellipticity values ($[\theta]_{mrw}$) were calculated using the expression:

$$[\theta]_{mrw}(\text{deg}\cdot\text{cm}^2/\text{dmol}) = 100\theta_{obs}/lc$$

where $\theta_{obs}$ is the observed ellipticity in degrees, $c$ is the molar residue concentration, and $l$ is the light path in cm.

*ANS-Binding Fluorescence.* ANS was purchased from Sigma (St. Louis, MO) and further purified by recrystalization twice as described by Weber and Young (*26*). The ANS concentration was determined spectrophotometrically using the extinction coefficient $4.95 \times 10^3$ $M^{-1}$ $cm^{-1}$ at 350 nm. The fluorescence instrument was an SLM model 8100 spectrofluorometer upgraded with computer control. The sample contained 30 $\mu$M ANS, 2.7 $\mu$M protein, 300 mM NaCl, and 50 mM $CaCl_2$. The emission spectra were obtained at 37 °C by collecting emission fluorescence from 400 to 600 nm with excitation at 390 nm.

## RESULTS

*The Structural Perturbation Is pH- and Mutation-Dependent.* Most of our previous NMR analyses were performed at pH* 4.0. To investigate pH effect, we have now performed 1D and/or 2D $^1$H NMR analyses for some of the mutants at different pH* (from pH* 8 to pH* 1). The results indicate that the "global structural perturbation" or the formation of the "molten globule-like state," as described in previous studies (e.g., *9*), is a pH-dependent phenomenon. The mutants I9Y and I9F show perturbed NMR properties throughout the pH range studied; the representative NOESY spectra at pH* 7.0 are shown in Figure 2. The mutants H48A and C44A/C105A (a double mutant with a disulfide bond deleted), on the other hand, display native-like spectra at neutral pH* and molten globule-like spectra at acidic pH*, as shown by the 2D NOESY spectra of H48A (Figure 3). The corresponding spectra of C44A/C105A are similar to those of H48A and are thus not presented. For the mutants in this category, a "transition pH" from the native-like state to the molten globule-like state can be clearly identified, as illustrated by the 1D NMR spectra of C44A/C105A in Figure 4. The spectra in Figure 4 show that from pH* 7.8 to 4.5 there are small changes due to the pH effect, but the overall resonances remain sharp and well dispersed. Line broadening occurs at pH* 4.0 and becomes severe at pH* 3.5. When the sample was titrated back to pH* 7.1, the native-like spectrum was fully recovered, indicating that the acid-induced effect is reversible. The H48A mutant displays a similar behavior with a transition pH* around 4.0. On the other hand, WT PLA2 is able to retain its native-like structure except under highly acidic conditions such as 1 M HCl, as described in a later section.

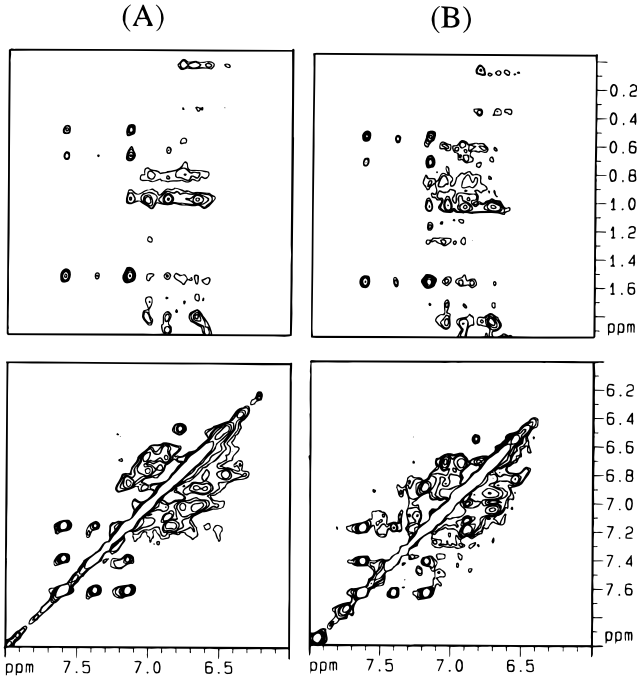


FIGURE 2: Partial NOESY spectra of I9Y (A) and I9F (B) at pH* 7.0, recorded in $D_2O$ at 37 °C. For comparisons, see Liu et al. (*7*) for the NOESY spectra of these two mutants at pH* 4.0.

*Characterization of the Molten Globule-like State of H48A by CD and Fluorescence.* The results described in the previous section, as well as related results described in previous publications, are mainly based on $^1$H NMR studies. In what have become routine methods in the study of molten globules, CD and fluorescence are usually employed to follow the conformational changes.

H48A was used to rigorously establish the property of the molten globule-like state of PLA2 mutants. One of the key properties of a classical molten globule state is that it loses the tertiary structure while retaining the secondary structure (*14*). It has been well-established that the far-UV CD spectrum of a protein reflects its secondary structure, whereas the near-UV CD spectrum reflects its tertiary structure (*27*). As shown in Figure 5A, the far-UV CD spectra of H48A remain largely unchanged from pH 7.0 to pH 0.7, suggesting that H48A retains a high degree of native-like secondary structure throughout the entire pH range. The spectra are in agreement with ca. 45% α-helical content. On the other hand, the near-UV CD spectra shown in Figure 5B display

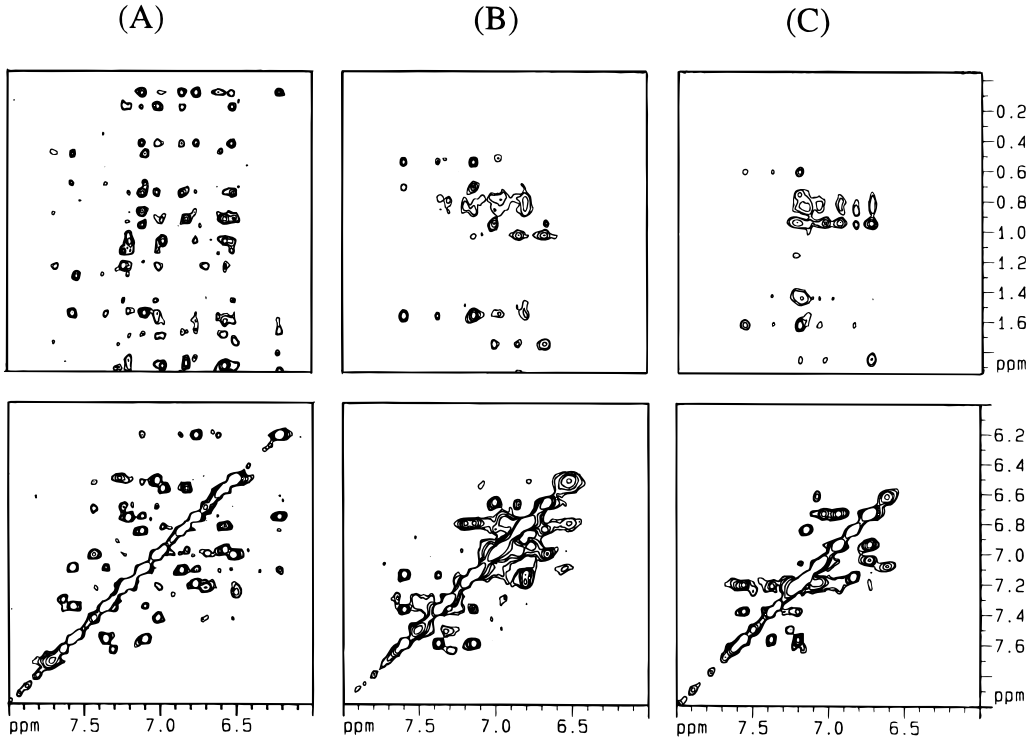


FIGURE 3: Partial NOESY spectra of H48A at pH* 7.0 (A), 3.8 (B), and 1.3 (C), recorded in $D_2O$ at 37 °C.

significant changes between pH 4.9 and 2.0, characteristic of a loss of the tertiary structure.

Fluorescence is another useful tool. However, the fact that the only tryptophan is solvent-exposed in PLA2 necessitated the use of ANS as an extrinsic probe. The important characteristic of the molten globule state is that it shows enhanced binding of ANS due to enhanced accessibility (or exposure) of the hydrophobic core of the protein (*14*). The emission maximum of ANS is at 515 nm with a low quantum yield. The fluorescence curves of pure ANS are almost identical in the entire pH range studied. When it binds H48A at neutral pH, the fluorescence intensity is increased considerably and the peak is blue-shifted to around 480 nm (Figure 6, curves a and b). As shown in Figure 6, the fluorescence intensity of ANS is further enhanced substantially from pH 4 to pH 3, suggesting a transition to the molten globule-state. In agreement with the NMR experiment shown in Figure 4, the ANS-binding fluorescence experiment (data not shown) also indicates that the native-to-molten globule transition induced by pH is a reversible process.

In Figure 7, near-UV CD signals at 282.4 nm and relative fluorescence intensities at 484 nm are plotted against pH. The transition pH was estimated to be 3.4 by fitting the ellipticity changes at 282.4 nm to a two-state model (native state ⇔ molten globule-like state). This result provides further support to the NMR results described in the previous section.

*Retention of Some Rigid Tertiary Interactions in the Molten Globule-like State.* The classical molten globule is known for its complete disruption of rigid packing and thus the loss of rigid tertiary interactions (*14*, *15*). However, analyses of 2D NOESY spectra suggested the retention of some rigid tertiary interactions in our molten globule-like states, as explained below.

There are one Trp, four Phe, and seven Tyr residues in bovine pancreatic PLA2. At neutral pH, H48A and C44A/C105A mutants displayed native-like chemical shifts of aromatic spins (Figure 3A). When pH was lowered to acidic conditions, conformational changes were immediately apparent in 2D NOESY spectra. For example in Figure 3B recorded around pH 3.7, NOEs were fewer in number, more poorly dispersed, and of lower intensity. One of the most noticeable features was that signals around 0 ppm, assigned to I9 and L41, were reduced to the noise level. The side chains of these two residues display extensive NOEs to F22 (from I9 and L41), F106 (from I9 and L41), and Y111 (from L41) in the native state (*1*). The loss of these NOEs coupled with the loss of the characteristic chemical shifts of these aromatic spins (e.g., $H^{\epsilon}$ of Y111 ∼ 6.15 ppm) strongly signified disruption of the tertiary structure in the lower half of the protein (in reference to the structure shown in Figure 1).

On the other hand, a set of interresidue NOE cross-peaks is retained in the molten globule-like states, as shown in Figures 2 and 3B. The unique chemical shifts of F94 allowed unambiguous assignments of the cross-peaks of $H^{\beta}$(A55)/$H^{\delta,\epsilon}$(F94), $H^{\beta}$(Q54)/$H^{\epsilon,\zeta}$(F94), and $H^{\delta1,\delta2}$(L58)/$H^{\delta,\epsilon}$(F94), indicating strong contacts between helices II and IV. Another four pairs, $H^{\gamma2}$(I95)/$H^{\delta,\epsilon}$(Y73), $H^{\gamma11}$(I82)/$H^{\delta,\epsilon}$(Y75), $H^{\epsilon}$(M8)/$H^{\delta,\epsilon}$(Y73), and $H^{\epsilon}$(M8)/$H^{\delta,\epsilon}$(Y75), are tentatively assigned in H48A (see the Supporting Information) but are also likely to appear in other mutants (*5*−*13*). Interestingly, all of the residues involved and the $\epsilon$-$CH_3$ of M8 are situated in the upper half in Figure 1.

*Retained Tertiary Interactions Are Localized in the Upper Half of the Structure.* The H48A sample was used to further map the structured residues in the molten globule-like state through the analysis of backbone amides. Figure 8 provides qualitative comparisons of amide regions between H48A and WT and between different pH values for each sample. The detailed analysis of H48A was achieved by means of heteronuclear NMR experiments on a uniformly $^{15}N$-labeled

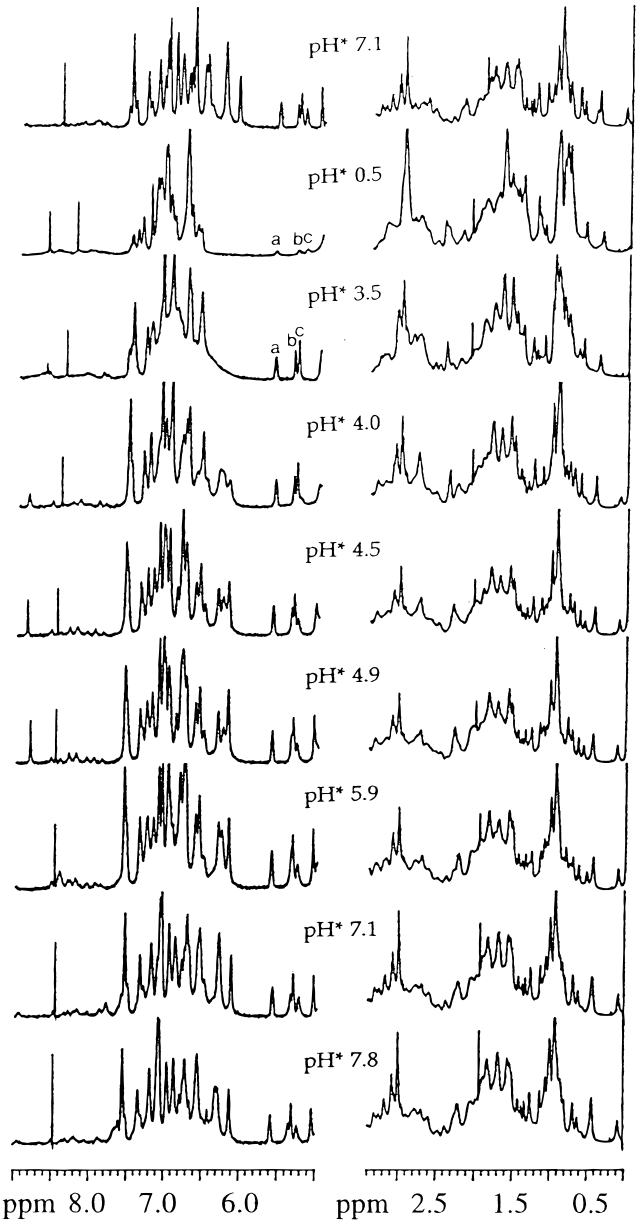


FIGURE 4: 1D $^1H$ NMR spectra of C44A/C105A as a function of pH*, recorded in $D_2O$. The top spectrum at pH* 7.1 was recorded by titrating the sample back from pH* 3.5. The peaks marked with a, b, and c in the spectra recorded at pH* 3.5 and 0.5 have been assigned to the $H^\alpha$ resonances of C77, Y75, and S74, respectively.

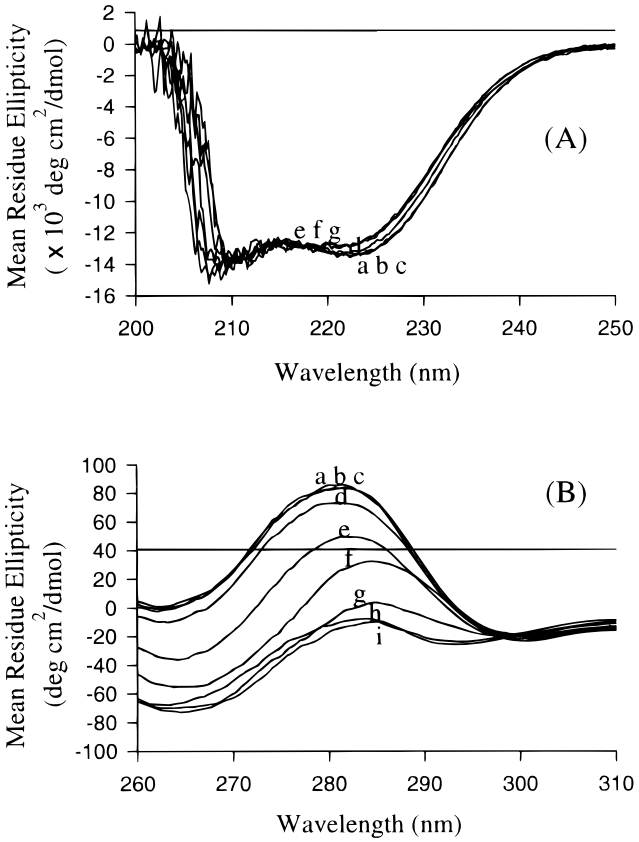


FIGURE 5: CD spectra of H48A. Details of data collection are given in the text. We reduced the concentration of salts (NaCl and $CaCl_2$) in the far-UV CD experiments because the $Cl^-$ ion interferes with the measurements. (A) Far-UV CD at the following pH: (a) 7.0, (b) 6.0, (c) 5.1, (d) 4.0, (e) 3.1, (f) 2.2, and (g) 1.0. (B) Near-UV CD as a function of pH: (a) 7.8, (b) 6.7, (c) 5.8, (d) 4.9, (e) 4.0, (f) 3.0, (g) 2.0, (h) 1.0, and (i) 0.6.

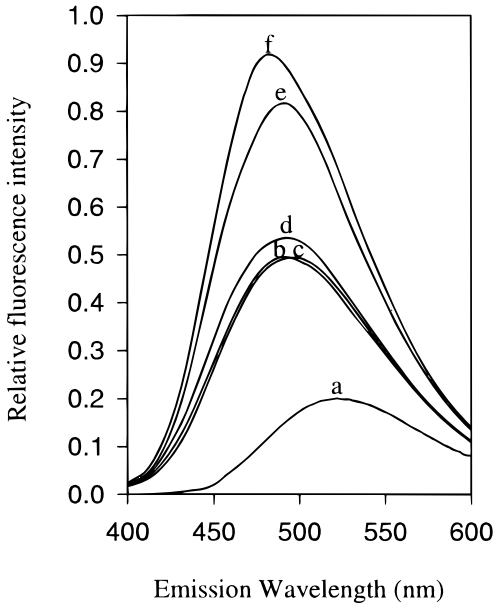


FIGURE 6: Fluorescence emission spectra of ANS (a) in the absence of H48A, pH 6.9; (b−f) in the presence of H48A, pH 6.9 (b), pH 5.0 (c), pH 4.0 (d), pH 3.1 (e), and pH 2.7 (f). The spectrum of pure ANS in the buffer does not change in the entire pH range. Details of data collection are given in the Materials and Methods.

sample. Experiments such as 2D HSQC and 3D NOESY-HSQC were carried out at pH 6.0 and 4.0. At pH 6.0, the sample produces a well-dispersed $^1H-^{15}N$ correlation spectrum (Figure 9). All but 9 of the 119 possible backbone amides were assigned on the basis of the WT assignments (*1*). With the exception of A48 and its neighboring residues (e.g., D99, Y52, and A102), most of the backbone amides have chemical shifts similar to those in WT. Therefore, the conformational changes between H48A and WT are only localized.

When the pH was lowered to 4.0, the changes in the amides were dramatic. First, the peaks in the HSQC spectrum became broad and poorly resolved, especially in the region roughly defined by $^{15}N$ 115−125 ppm and $^1H$ 7.7−8.7 ppm (Figure 10). A set of well-dispersed $^1H-^{15}N$ cross-peaks in the native state, such as C27, Y28, G35, V38, N112, and C123, was found missing or probably was broadened out to the extent of being undetectable. Second, there was substantial loss of amide-related NOEs in NOESY spectra (e.g.,

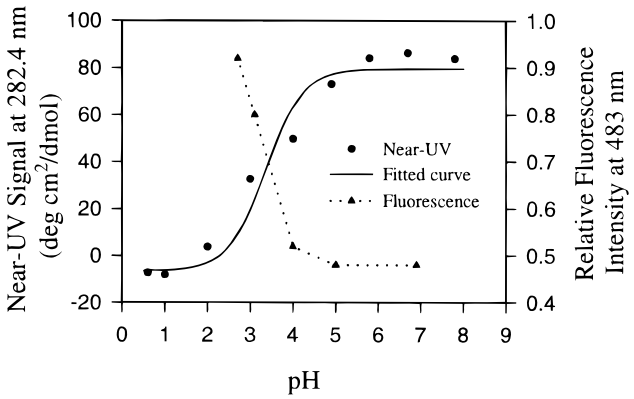


FIGURE 7: Near-UV CD signals at 282.4 nm and relative fluorescence intensities at 484 nm are plotted against pH. The transition pH was estimated at pH 3.4 by fitting the ellipticity changes at 282.4 nm to a two-state model (native state ⇔ molten globule like state).

Figure 8B), including those characterizing secondary structures such as NN(i, i+1). These observations can be attributed to a rapidly interconverting mixture of different populations in the molten globule-like state, by which the severe exchange broadening results in the missing of $H^N$ peaks (*28*). However, in accord with the analyses in the aromatic−aliphatic region, the protein was not completely unstructured. There existed a reasonable amount of interresidue NOEs, including some connectivities reflecting the persistent secondary elements. Table 1 in the Supporting Information lists the interresidue NOEs that have been assigned in 3D $^1H-^{15}N$ NOESY-HSQC experiments. In summary, NN(i, i+1) stretches were found in the following segments: Q54−L58 (helix II), D59−V63 (helix III), and A90−C98 (helix IV), while medium and strong αN(i, i+1) were still observed in the $\beta$-wing (S74−N79 and E81−T83). The preservation of the $\beta$-wing was further supported by $H^N$(S78)/$H^N$(E81) NOE. On the other hand, these secondary structure elements are apparently not as well defined as their counterparts in the native state in terms of NOE number and intensity. For instance, the intensities of assigned sequential NN(i, i+1) NOEs are generally reduced in α-helices, while in the $\beta$-wing, the increased flexibility is clearly evidenced by the absence of $H^N$(S76)/$H^N$(S85) NOE.

In summary, most, if not all, of the connectivities in the molten globule-like state of H48A were found in the segment of 52−97. These residues also account for 38 of 41 amide cross-peaks assigned in HSQC (Figure 10), in which the side chain amides of Q54, N80, N88, and N97 are also well dispersed and do not show significant changes relative to native ones. Moreover, there exist tertiary interactions between helices II and IV and between helix IV and $\beta$-wing in the region defined by the above residues. All of these NMR data led to the suggestion of a partially structured molten globule-like state, despite that the structured part is obviously not as good as the counterpart in the native state.

Consistent with the conclusion reached from NMR analyses, we have noticed that the magnitudes in ANS fluorescence changes observed in Figure 6 are smaller than those observed for other molten globules (e.g., *29*). Also, the near-UV CD peaks in Figure 5B do not completely disappear after the transition.

*The Retained Tertiary Structure Could Be Stabilized by Disulfide Bonds.* Figure 11 shows a stereodiagram of a PLA2 solution structure with assigned amides labeled and with the side chains of M8, Q54, A55, L58, Y73, Y75, I82, F94, and I95 highlighted. It is obvious that the assigned residues group in the upper half. While present data do not allow us to pinpoint the origin of stabilization forces, close examination of Figure 11 suggests a potential effect from disulfide bonds. C91−C61 and C98−C51 could plausibly provide support for the tertiary interaction between helices II and IV and between helices III and IV in the upper half of the enzyme, while C84−C96 may be attributed to the stabilization of interaction between $\beta$-wing and helix IV. The disulfide bond of C11−C77 may also make some contributions. This proposition, however, does not rule out the contribution from other long-range interactions.

*Acid Cannot Completely Unfold the Mutants.* Acid is weak in denaturing capacity compared with other denaturing agents such as guanidinium chloride and urea (*30*). Among many different acids, HCl is the choice to check the maximum acid-induced unfolding because it has the poorest ability to stabilize the intermediate state (*31*). In this work, it was found that H48A and C44A/C105A mutants could not fully unfold in the pH range studied: between pH 7.3 and 0.5.

The drastic conformational changes occurred around pH 4.0 for H48A and C44A/C105A mutants. From there and down to ∼ pH 0.5, the changes in conformation are gradual rather than dramatic on the basis of the observations in NMR and CD. What was observed in this pH range can be summarized as follows: (1) The protein keeps losing tertiary structure as revealed by near-UV CD and 2D NOESY, but the side chain−side chain NOEs of Q54/F94, A55/F94, and L58/F94 are still visible in 2D NOESY recorded at acidic pH (Figure 3C), which indicates strong interactions between helices II and IV. (2) A significant amount of secondary structure is still preserved as evidenced by far-UV CD (Figure 5A). However, the $\beta$-sheet starts to lose its structure probably around pH 2.0, as signified by a gradual decrease in the resonance intensities of three downfield α protons (S74, Y75, and C77), which are indicative of structured $\beta$-strands. These peaks are barely visible at pH* 0.5 in C44A/C105A mutant (Figure 4, spectra at pH* 3.5 and 0.5).

*Wild-Type PLA2 Exhibits Exceptional pH Stability.* While the results described above show that the structure of PLA2 can easily be perturbed by certain site-specific mutations and that the structural perturbation of some of the mutants is induced by weak acid, WT PLA2 displays well-resolved $^1H$ NMR resonances even at pH* 2 or 3, as shown by the pH titration experiment of 1D $^1H$ NMR (Figure 12). Only when concentrated DCl was added (e.g., titrated to around pH* 0) did the protein give broad NMR resonances and lose NOE cross-peaks as significantly as did those mutants in molten globule-like state (top spectrum in Figure 12). Although only the spectra at six different pH values are shown in Figure 12, separate detailed titration experiments have been performed with 24 different pH* values ranging from 1.9 to 9.2 (spectra not shown). In addition, 2D NOESY experiments have been performed at selected pH*: 7.1, 3.9, and 0 in $D_2O$ (Figure 13), and at pH 6.0 and 4.0 in $H_2O$ (Figure 8C,D). It is of importance to note the distinct similarity between Figure 13C and the NOESY spectra of mutants in the molten globule-like state. For example, the NOEs of Q54/F94, A55/F94, and L58/F94 can be unequivocally assigned

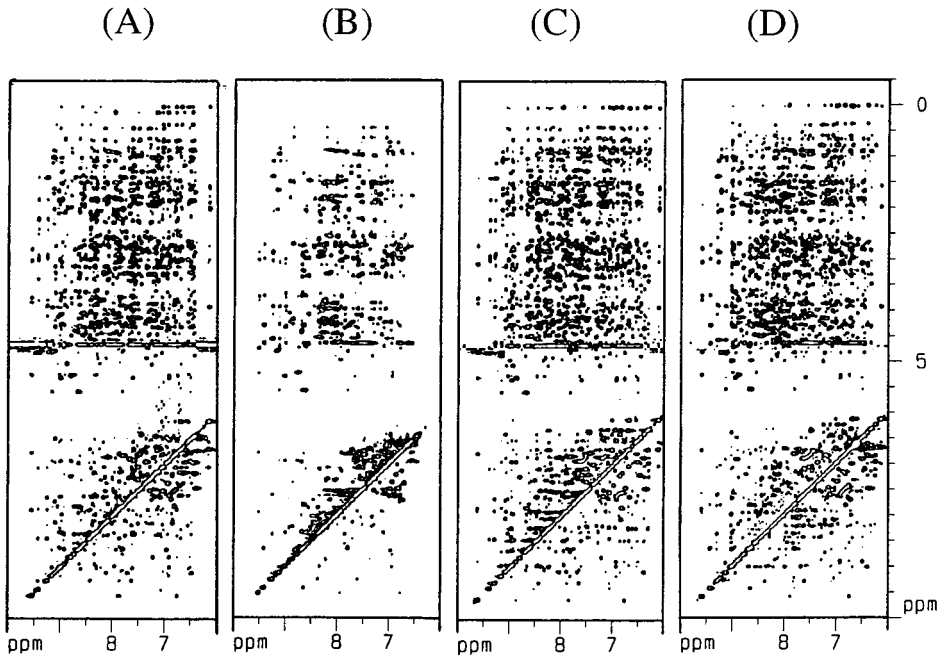


FIGURE 8: Partial 2D NOESY spectra recorded in $H_2O$ showing the amide region: (A) H48A at pH 6.0; (B) H48A at pH 4.0; (C) WT at pH 6.0; and (D) WT at pH 4.0.

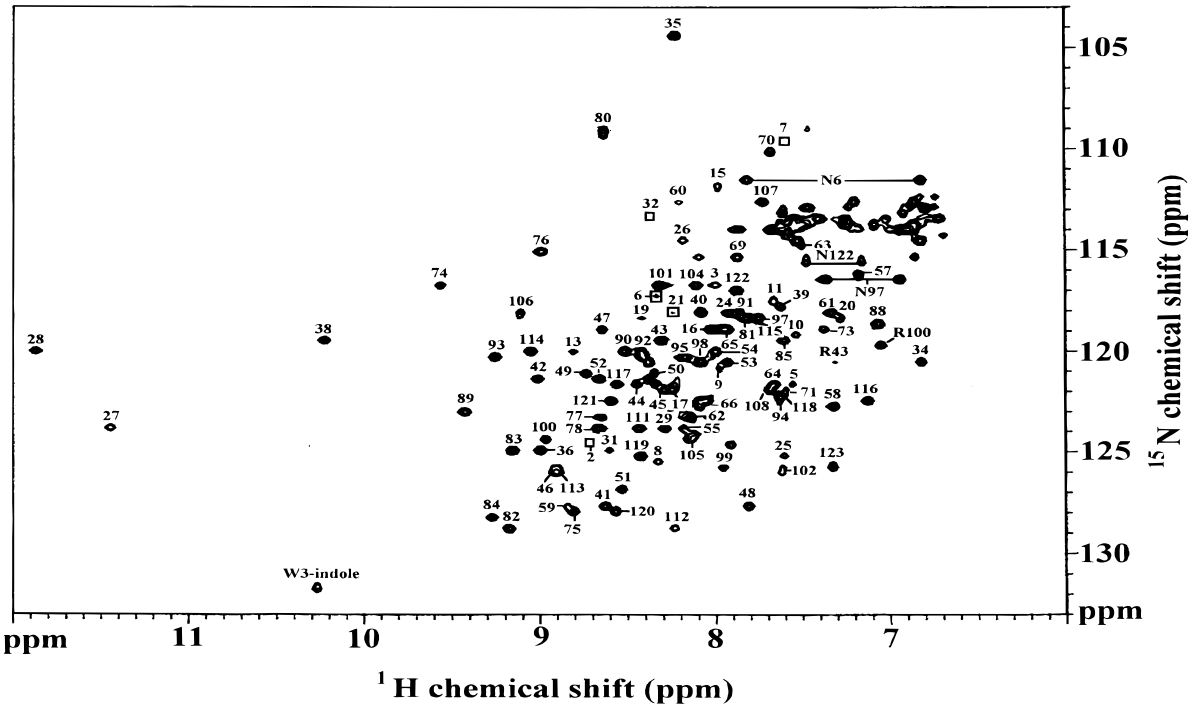


FIGURE 9: $^{1}H-^{15}N$ HSQC spectrum recorded in $H_2O$ at pH 6.0 on the $^{15}N$-labeled H48A sample. 110 out of 119 possible backbone amides have been assigned.

and the NOEs of I9 and L41 are mostly lost (Figure 13C). However, we have not performed more experiments to characterize the transition to and the nature of the molten globule-like state for WT PLA2 because concentrated HCl and salts are unfavorable for CD, fluorescence, and NMR experiments.

Nevertheless, our results are sufficient to indicate that WT PLA2 is acid stable, retains native structure at least under mildly acidic conditions, and is probably converted to a molten globule-like state only at extreme pH (e.g., after addition of 1 M HCl).

## DISCUSSION

*pH-Induced Conformational Changes of PLA2.* H48A was selected for a thorough study in this work by a combination of CD, fluorescence, and NMR because of its catalytic significance and intriguing structural properties. The conclusions reached from this mutant presumably can be extended to other mutants and WT. On going to the molten globule-like state, the tertiary packing is disrupted while the secondary structure is mostly retained. The protein experiences increased structural flexibility in a heterogeneous manner rather than a uniform melting. Specifically, the lower

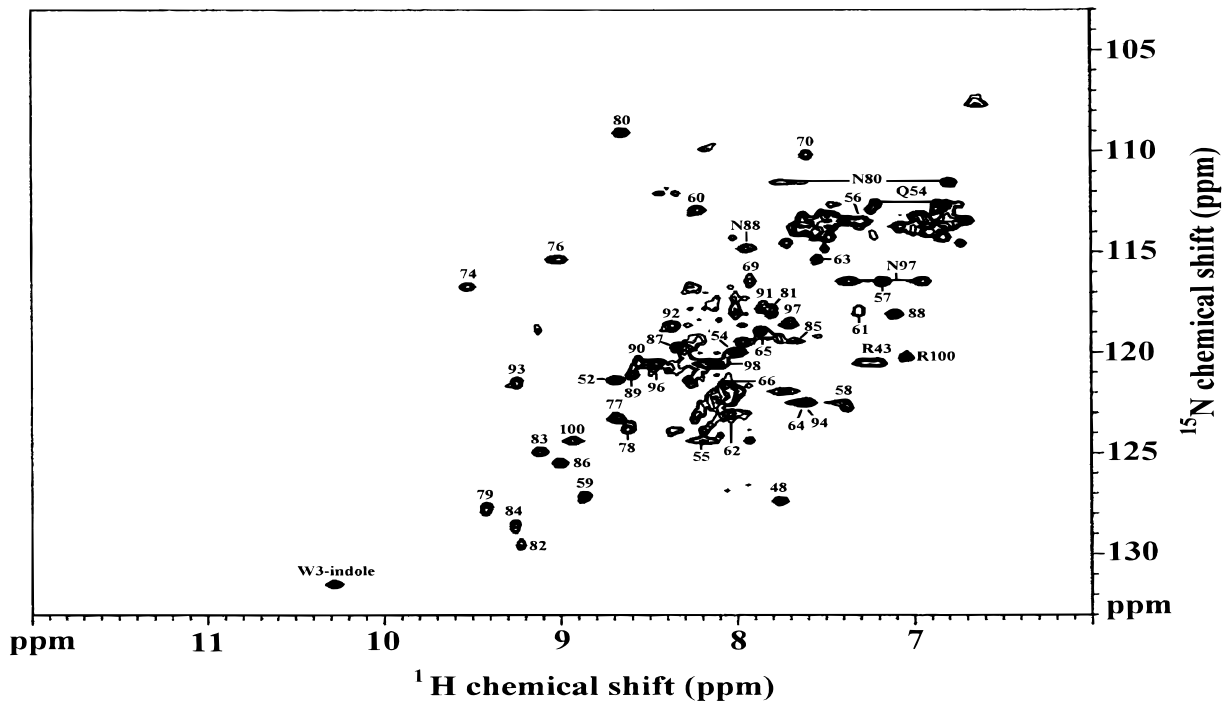


FIGURE 10: $^{1}H-^{15}N$ HSQC spectrum recorded in $H_2O$ at pH 4.0 on the $^{15}N$-labeled H48A sample. Only 41 backbone amides could be assigned.

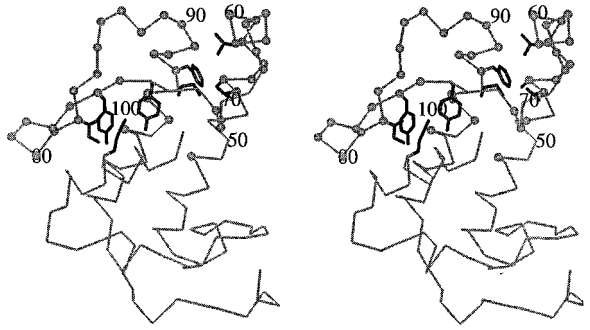

FIGURE 11: Stereodiagram of the PLA2 solution structure (α-carbon trace) showing the side chains (heavy line) assigned in the NOESY spectrum and the backbone amides (gray dots) assigned in the HSQC spectrum for H48A mutant at pH 4.0. It is obvious that these residues are grouped in the upper half. The four disulfide bonds (C51−C98, C61−C91, C84−C96, and C11−C77) could be responsible for the retention of partial tertiary structure.

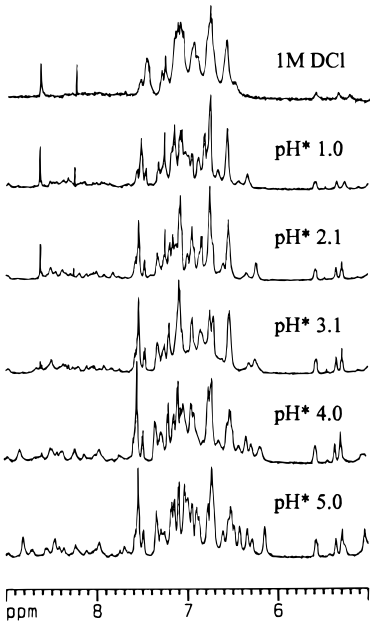


FIGURE 12: 1D $^{1}H$ NMR spectra of WT PLA2 as a function of pH*, recorded in $D_2O$ at 37 °C.

half of the protein with extensive hydrophobic interactions involving I9, F22, L41, F106, and Y111 loses its tight packing at the onset of unfolding, whereas the upper half remains relatively structured. On approaching extreme pH, the tertiary structure becomes less ordered but rigid contacts still exist to some extent between helices II and IV. Meanwhile, the $\beta$-wing starts to lose its secondary structure. It should be noted that the transition to a molten globule-like state induced by pH must be accompanied by the release of calcium ions because the binding loop becomes disordered.

In acid denaturation, intramolecular charge repulsion is the driving force for unfolding. The protonation of certain residues involved in critical interactions could trigger the onset of unfolding, resulting in a melting of tertiary packing (*32*). For H48A and C44A/C105A mutants, the likely candidates for protonation could be confined to one or more of His, Asp, and Glu residues, whose p$K_a$ can be somewhere around pH 4.0. Structural inspection suggested D39 as a possible candidate, whose side chain pointing inside is engaged in interactions with several residues in the lower half of the protein.

It remains to be established why some of the mutants are so susceptible to acid-induced changes. While these problems are subjects for further investigation, one possibility is that the conformational transition could be triggered by the release of calcium ions. However, this would require a p$K_a$ perturbation in the side chain of D49, the calcium binding residue, between WT and mutants. Furthermore, D49 mutants do not exist in a molten globule state at pH 4.0 (*33*). Thus, while calcium release must accompany the formation of the molten globule-like state, it does not appear to trigger the event.

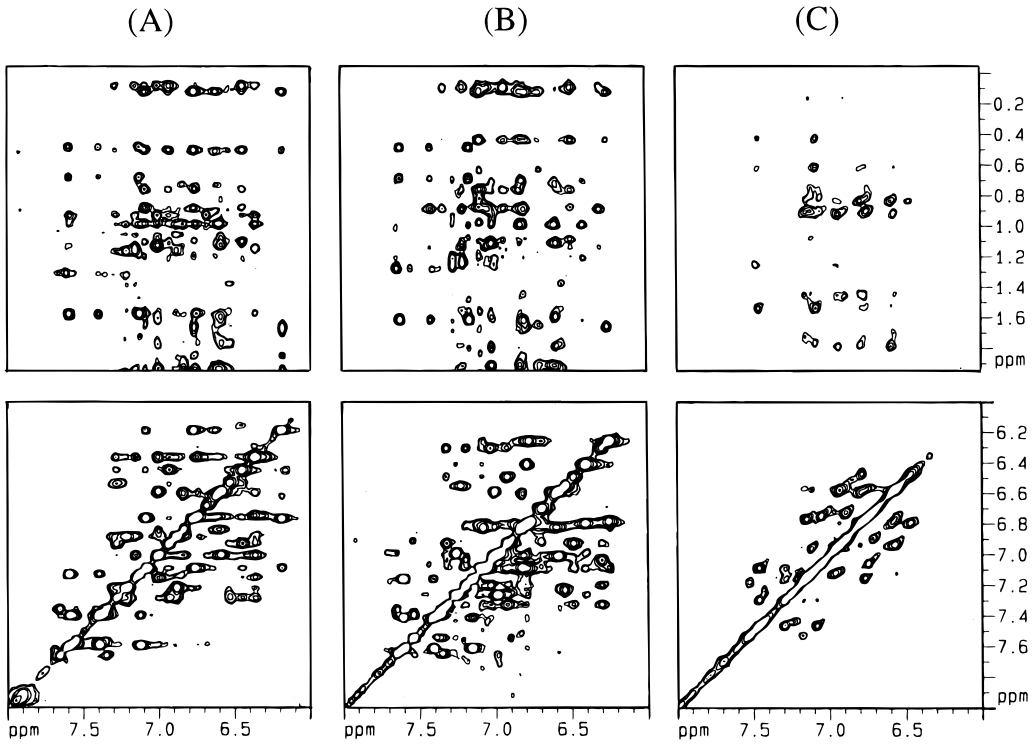


FIGURE 13: Partial NOESY spectra of WT at (A) pH* 7.1, (B) pH* 3.9, and (C) in the presence of 1 M DCl, recorded in $D_2O$ at 37 °C.

An important point of clarification is that we have not stated or assumed that there is no structural change prior to the global conformational transition. For example, even though WT PLA2 was able to retain its native-like state over a wide range of pH, this does not mean that there no structural changes in that range. There must be some local changes, as evidenced by the small changes of the 1D $^1$H NMR spectra observed in the detailed pH titration experiments and subtle differences in 2D NOESY experiments (Figures 8C vs 8D, and 13A vs 13B). Moreover, the calcium ion is likely released from PLA2 at acidic pH (*34*). These local changes also warrant detailed investigation because they are obviously functionally relevant.

*A Stable* $\boldsymbol{\beta}$*-Sheet and Fluctuating* $\alpha$*-Helices?* In terms of hydrogen−deuterium exchange rate, α-helix IV is regarded as the most stable secondary element in WT PLA2, followed by α-helix II. For instance, HSQC recorded after 6 days of exchange at 37 °C only revealed 10 residues, all in helix IV (C96, N97, C98, D99, R100, N101, A102, A103, I104, and F106) (*1*). Interestingly, both helices are only partially structured in the molten globule-like state of H48A. Furthermore, the retained structure in helix IV consists of a different set of residues: A90−N97. Whether structured or not, the helices overall are becoming fluctuating. This may be visualized through a theoretical simulation on the unfolding of hen egg-white lysozyme (*35*), in which the main chain C═O and H−N groups in the helices quickly alternate between bonding with each other and with nearby water molecules in the molten globule state.

The $\beta$-wing, in contrast, has a less perturbed structure. First, most of the amides in the $\beta$-wing could be observed in HSQC at pH 4.0. Second, their chemical shifts, as well as those of α protons, remain well dispersed and almost unchanged (see the Supporting Information). Third, the αN connectivities and $H^N$(S78)/$H^N$(E81) NOE are still retained. These data thus provide compelling evidence that the highly ordered antiparallel $\beta$-wing is populated in the molten globule-like state of H48A. In addition, the $\beta$-wing can sustain strong acid before losing its structure, as mentioned above. This relative persistence of the $\beta$-sheet could be attributed to the stabilization by its enriched and mostly solvated polar side-chains.

Despite generally poor sequence conservation in this segment, all known class I and class II PLA2 structures contain one well-developed $\beta$-wing (*36*). Because of its lack of functional residues, the $\beta$-wing has received little attention in structure−function relationship studies. The role of this segment should be to maintain PLA2 structural integrity through the Y73−D99 hydrogen bond between the $\beta$-wing and helix IV and the C77−C11 disulfide bond between the $\beta$-wing and helix I. The importance of these two interactions to structure has been confirmed by mutagenesis (*10*, *12*).

*Comparisons with Other Proteins.* Molten globule states have been characterized by significant structural variability, ranging from highly unfolded to near native-like structures (*15*). In recent years, several proteins were shown to acquire a partially folded state, sometimes called the A-state. For example, the molten globule structures of apocytochrome $b_{562}$ (*37*) and interleukin-4 (*38*) are both highly ordered compared to most other molten globule states. Also, in the globule acidic form of cytochrome *c* (*39*), the major helices of cytochrome *c* and their common hydrophobic domain are largely preserved while the loop region of the native structure is flexible and partially disordered.

Although many proteins become molten globules only at extreme pH such as pH 2.0, it has been observed for other proteins to undergo global changes under mild conditions. For example, a fully active mutant of human interleukin-6 (*40*) was reported with the transition midpoint of pH $\sim$ 4.5, and it was suggested that Glu and/or Asp residues are

responsible for this conformational transition. That midpoint shift in pH changes from WT to mutants, presumed to reflect the changes in stability of the native and intermediate states, has also been observed in apomyoglobin, investigated by Baldwin and co-workers (*41*, *42*). Interestingly, the midpoint of pH 4.0 in WT was caused by a perturbed p$K_a$ of one buried His residue. Mutation on this site was shown to stabilize the native state, shifting the midpoint of native ⇔ intermediate to lower pH.

In another point, we attribute the structured upper half to the stabilization of several disulfide bonds. Similar attribution was also mentioned in the study of the molten globule state of bovine serum fetuin, which possesses quasi-intact secondary structures and some long-range interactions (*43*).

*Implications in Enzyme Evolution.* Many proteins demonstrate remarkable tolerance to amino acid substitutions (*44*). In other words, mutations are only accommodated by minor adjustments of protein structure without substantial decrease in the overall stability. This plasticity is well exemplified by adenylate kinase (AK), a protein that has no disulfide bonds and is only marginally stable ($\Delta G_d^{H_2O} = 3.8$ kcal/mol) (*45*). Among the more than 50 mutants that have been characterized in our group, most, if not all, show only minor changes in the NMR properties and in the conformational stability relative to WT (*45*). By contrast, the rigid and stable PLA2 structure appears fragile; mutants are comparatively easily induced into a molten globule-like state. Although structural perturbations caused by single mutations also occur with other proteins, the frequency of occurrence and the extent of perturbation in PLA2 are unprecedented, which is particularly unexpected in view of the extreme heat and acid stability of WT PLA2. The behavior of PLA2 can be interpreted as "stable but fragile," while AK can be said to be "unstable but flexible." One could draw an analogy that PLA2 and AK are like glass (hard and fragile) and rubber (soft and flexible), respectively.

The fragile sites in PLA2 include two key catalytic residues, H48 and D99. It is well-known that D99···H48···$H_2O$ is the catalytic triad in PLA2. However, our work (*1*, *6*, *9*, *10*) has led to an important finding of the structural role of another triad Y73···D99···H48, which could be crucial for the enzyme's structural integrity as well as stability. The dual role of the D99···H48 dyad illustrates an important point in enzyme evolution: As a primitive enzyme improves its catalytic efficiency under the evolutionary pressure, it also has to take care of the possible structural perturbation caused by mutations. Likewise, when the enzyme evolves its tertiary structure, it has to optimize both the structure and the function. In other words, enzyme evolution involves the interplay between structure and function. At this stage, PLA2 structure probably has been nearly "perfect," especially around the active site; thus a single mutation is likely to disrupt this perfect structure.

The biological significance of fragility in the PLA2 structure needs further investigation. It is particularly interesting to note that the fragile lower half has more functional residues than the upper half. The active site (H48···D99), the hydrophobic channel, the putative interfacial binding site, and the calcium-binding loop, are mainly situated in the lower half.

*Potential Significance in Protein Folding and Protein Design.* The characterization of unfolded and partly folded states of proteins is central to understanding protein stability and folding, as well as providing a basis for protein design. There is growing evidence that the molten globule states may resemble folding intermediates and a residual structure in the denatured state may contain clues to folding events (*15*). One specific example is apomyoglobin investigated by Wright, Dyson, and co-workers (*46*, *47*), whose NMR work demonstrated that pH-dependent partially folded molten globules are likely to occur during folding of myoglobin.

Protein folding is beyond the scope of this paper. Nevertheless, the work presented here might have some implications on this subject. First, molten globules are usually observed under highly denaturing conditions such as extreme pH, high temperature, or moderate concentration of denaturant. Our results suggest that the condition can be softened by appropriate mutagenesis in this regard. Second, it was suggested that "highly ordered molten globules" are likely to resemble the structures occurring late in the protein folding process (*48*). The molten globule-like state of PLA2 can also plausibly correspond to on-pathway folding intermediates. That the very different mutants H48A and C44A/C105A bear similarity in the pH-induced unfolding state could suggest that the folding at the final stage involves tuning of tertiary interactions mostly in the lower half of the molecule.

The main incentives to protein design have been to test our understanding of protein structure and to design a novel protein possessing therapeutically or industrially important activities (*49*). The past two years have observed a major advance in de novo protein design accomplished by several groups (*50*, *51*). It appears surprisingly easy to obtain globally correct folds. However, the difficulty still exits in designing well-ordered cores (*52*), let alone designing novel proteins for pharmaceutical applications. The likelihood of success will be enhanced ultimately by progressive design and iterative cycles. Further interplay between structure and function will be especially important in view of potential designed pharmaceutical enzymes. The detailed study on PLA2 potentially could provide very useful information in this respect.

## ACKNOWLEDGMENT

We are indebted to Dr. D. Pfeiffer at The Ohio State University for making his fluorimeter available to us and to Dr. E. Wang for assisting us in the fluorescence experiments.

## SUPPORTING INFORMATION AVAILABLE

Two tables and one figure containing the intraresidue NOE assignment in 3D $^1H-^{15}N$ NOESY−HSQC on H48A mutant at pH 4.0 (Supplementary Table 1), chemical shift assignments of amides and $H^\alpha$ protons for $\beta$-wing of H48A at pH 6.0 and pH 4.0 (Supplementary Table 2), and a sample of NOE assignment in H48A mutant at mildly acidic pH (Supplementary Figure 1). This information is available free of charge via the Internet at http://pubs.acs.org.

## REFERENCES

1. Yuan, C.-H., Byeon, I.-J. L., Li, Y., and Tsai, M.-D. (1999) *Biochemistry 38*, 2909−2918.
2. Dijkstra, B. W., Drenth, J., Kalk, K. H., and Vandermaelen, P. J. (1978) *J. Mol. Biol. 124*, 53−60.
3. Dijkstra, B. W., Kalk, K. H., Hol, W. G. J., and Drenth, J. (1981) *J. Mol. Biol. 147*, 97−123.

4. Fisher, J., Primrose, W. U., Roberts, G. C. K., Dekker, N., Boelens, R., Kaptein, R., and Slotboom, A. J. (1989) *Biochemistry 28*, 5939−5946.
5. Dupureur, C. M., Yu, B.-Z., Mamone, J. A., Jain, M. K., and Tsai, M.-D. (1992) *Biochemistry 31*, 6402−6413.
6. Dupureur, C. M., Li, Y., and Tsai, M.-D. (1992) *J. Am. Chem. Soc. 114*, 2748−2749.
7. Liu, X.-H., Zhu, H.-X., Huang, B.-H., Rodgers, J., Yu, B.-Z., Kumar, A., Jain, M.-K., Sundaralingam, M., and Tsai, M.-D. (1995) *Biochemistry 34*, 7322−7344.
8. Zhu, H.-X. (1995) Ph.D. Dissertation, The Ohio State University, Columbus, OH.
9. Li, Y., and Tsai, M.-D. (1993) *J. Am. Chem. Soc. 115*, 8523−8526.
10. Dupureur, C. M., Yu, B.-Z., Jain, M. K., Noel, J. P., Deng, T., Li, Y., Byeon, I.-J. L., and Tsai, M.-D. (1992) *Biochemistry 31*, 6402−6413.
11. Dupureur, C. M. (1992) Ph.D. Dissertation, The Ohio State University, Columbus, OH.
12. Zhu, H.-X., Dupureur, C. M., Zhang, X.-Y., and Tsai, M.-D. (1995) *Biochemistry 34*, 15307−15314.
13. Liu, X.-H. (1996) Ph.D. Dissertation, The Ohio State University, Columbus, OH.
14. Ptitsyn, O. B. (1992) in *Protein Folding* (Creighton, T. E., Ed.), pp 243−300, Freeman, New York.
15. Ptitsyn, O. B. (1995) *Curr. Opin. Struct. Biol. 5*, 74−78.
16. Fink, A. L., Calciano, L. J., Goto, Y., Kurotsu, T., and Palleros, D. R. (1994) *Biochemistry 33*, 12504−12511.
17. Plaxco, K. W., and Dobson, C. M. (1996) *Curr. Opin. Struct. Biol. 6*, 630−636.
18. Dyson, H. J., and Wright, P. E. (1996) *Annu. Rev. Phys. Chem. 47*, 369−395.
19. Deng, T., Noel, J. P., and Tsai, M.-D. (1990) *Gene 93*, 229−234.
20. Muchmore, D. C., Mclntosh, L. P., Russel, C. B., Anderson, D. E., and Dahlquist, F. W. (1989) *Methods Enzymol. 177*, 44−73.
21. Piotto, M., Saudek, V., and Sklenar, V. (1992) *J. Biomol. NMR 2*, 661−665.
22. Kay, L. E., Keifer, P., and Saarinen, T. (1992) *J. Am. Chem. Soc. 114*, 10663−10665.
23. Grzesiek, S., and Bax, A. (1993) *J. Am. Chem. Soc. 115*, 12593−12594.
24. Sklenar, V., Piotto, M., Leppik, R., and Saudek, V. (1993) *J. Magn. Reson. 80*, 241−245.
25. Marrion, D., Ikura, M., Tschudin, R., and Bax, A. (1989) *J. Magn. Reson. 85*, 393−399.
26. Weber, G., and Young, L. B. (1964) *J. Biol. Chem. 239*, 1415−1423.
27. Woody, R. W. (1995) *Methods Enzymol. 246*, 34−71.
28. Shortle, D. R. (1996) *Curr. Opin. Struct. Biol. 6*, 24−30.
29. Redfield, C., Smith, R. A. G., and Dobson, C. M. (1994) *Nat. Struct. Biol. 1*, 23−29.
30. Jaenicke, R., and Rudolph, R. (1989) in *Protein Structure* (Creighton, T. E., Ed.), pp 191−223, IRL Press, Oxford, England.
31. Goto, Y., and Fink, A. (1994) *Methods Enzymol. 232*, 3−15.
32. Ghelis, C., and Yon, J. (1982) *Protein Folding*, pp 227−229, Academic Press, New York.
33. Li, Y., Yu, B.-Z., Zhu, H.-X., Jain, M. K., and Tsai, M.-D. (1994) *Biochemistry 33*, 14714−14722.
34. Fujii, S., Meida, M., Tani, T., Inoue, S., Iwama, S., Katsumura, S., and Ikeda, K. (1998) *Arch. Biochem. Biophys. 354*, 73−82.
35. Williams, M. A., Thorntorn, J. M., and Goodfellows, J. M. (1997) *Protein Eng. 10*, 895−903.
36. Scott, D. L. (1997) in *Venom Phospholipase A2 Enzymes: Structure, Function and Mechanism* (Kini, R. M., Ed.), pp 97−128, John Wiley & Sons, New York.
37. Feng, Y., Sligar, S. G., and Wand, A. J. (1994) *Nat. Struct. Biol. 1*, 30−35.
38. Redfield, C., Smith, R. A. G., and Dobson, C. M. (1994) *Nat. Struct. Biol. 1*, 23−29.
39. Arcus, V. L., Vuilleumier, S., Freund, S. M. V., Bycroft, M., and Fersht, A. R. (1994) *Proc. Natl. Acad. Sci. U.S.A. 91*, 9412−9416.
40. De Filippis, V., Polverino de Laureto, P., Toniutti, N., and Fontana, A. (1996) *Biochemistry 35*, 11503−11511.
41. Barrick, D., Hughson, F. M., and Baldwin, R. L. (1994) *J. Mol. Biol. 237*, 588−601.
42. Geierstanger, B., Jamin, M., Volkman, B. F., and Baldwin, R. L. (1998) *Biochemistry 37*, 4254−4265.
43. Wang, C., Lascu, I., and Giartosio, A. (1998) *Biochemistry, 37*, 8457−8464.
44. Alber, T. (1989) *Annu. Rev. Biochem. 58*, 765−798.
45. Tsai, M.-D., and Yan, H. (1991) *Biochemistry 30*, 6806−6818.
46. Jennings, P. A., and Wright, P. E. (1993) *Science 262*, 892−896.
47. Eliezer, D., Yao, J., Dyson, H. J., and Wright, P. E. (1998) *Nat. Struct. Biol. 5*, 148−155.
48. Riddihough, G. (1994) *Nature 367*, 98.
49. Regan, L. (1998) *Structure 6*, 1−4.
50. Dahiyat, B. I., and Mayo, S. L. (1997) *Science 278*, 82−87.
51. DeGrado, W. F. (1997) *Science 278*, 80−81.
52. Hellinga, H. W. (1997) *Proc. Natl. Acad. U.S.A. 94*, 10015−10017.
53. Koradi, R., Billeter, M., and Wüthrich, K. (1996) *J. Mol. Graphics 14*, 51−55.


BI9822123